Current-Voltage Curves of Atomic-Sized Transition Metal Contacts: An Explanation of Why Au is Ohmic and Pt is Not

S. K. Nielsen,[1] M. Brandbyge,[2] K. Hansen,[1] K. Stokbro,[2] J. M. van Ruitenbeek,[3] and F. Besenbacher[1,*]

[1] *Interdisciplinary Nanoscience Center (iNano), CAMP and Department of Physics and Astronomy, University of Aarhus, DK-8000 Aarhus, Denmark*

[2] *Mikroelektronik Centret (MIC), Technical University of Denmark, Building 345E, DK-2800 Lyngby, Denmark*

[3] *Kamerlingh Onnes Laboratory, Universiteit Leiden, P.O. Box 9504, 2300 RA Leiden, The Netherlands*

(Received 7 March 2002; published 22 July 2002)

We present an experimental study of current-voltage (I-V) curves on atomic-sized Au and Pt contacts formed under cryogenic vacuum (4.2 K). Whereas I-V curves for Au are almost Ohmic, the conductance $G = I/V$ for Pt decreases with increasing voltage, resulting in distinct nonlinear I-V behavior. The experimental results are compared with first principles density functional theory calculations for Au and Pt, and good agreement is found. The difference in conductance properties for Pt vs Au can be explained by the underlying electron valence structure: Pt has an open d shell while Au has not.

DOI: 10.1103/PhysRevLett.89.066804 PACS numbers: 73.23.Ad, 73.63.Rt

In recent years the continuing miniaturization of nanoscale electronic components and integrated circuits has given rise to a rapidly growing interest in both experimental and theoretical properties of atomic-sized contacts (ASCs) [1].

For a macroscopic metal contact the conductance ($G = I/V$) decreases continuously with the diameter of the constriction. When the contact reaches atomic size, this is, however, no longer the case. As the diameter becomes of the order of the Fermi wavelength, the conductance will in some metals take on integer values of the fundamental unit of conductance $G_0 = 2e^2/h$, where e is the electron charge and h is Planck's constant. This phenomenon is called quantized conductance (QC). By constructing conductance histograms from numerous conductance traces (100–10 000) the most frequently occurring values of G are revealed as peaks [2]. The first peak usually corresponds to the conductance of a monatomic contact [3], and for the alkaline and noble metals this peak is situated at $1G_0$. For these metals also the next few peaks are positioned close to integer values of G_0 [3–5]. Most other metals do, however, not exhibit QC [3].

ASCs can be formed experimentally using several different techniques of which the most utilized are the scanning tunneling microscope [2,5–9], the mechanically controllable break junction (MCBJ) [3,4,10–15], and mechanical relays [16,17].

Although Au ASCs have been studied extensively [3,5–13,17], only limited knowledge exists on the current-voltage (I-V) behavior of Au ASCs [7–11]. The first reported high-voltage ($V > 100$ mV) I-V curves were highly nonlinear as G increased rapidly with voltage [7,8]. These findings were, however, not in accordance with reported conductance histograms showing that the conductance peak positions were bias independent [17]. In a recent paper it was concluded that this inconsistency was related to the cleanliness of the ASCs and only under ultraclean conditions could linear I-V curves for Au be acquired [9]. For Pt, experiments on ASCs have been more sparse. Values of the conductance of monatomic contacts have been reported to vary between $1.0G_0$ and $2.5G_0$ [2,6,13–16]. Conductance values close to $1G_0$ are, however, most likely caused by impurities, e.g., hydrogen [15,16]. No results exist on the I-V dependence.

In this Letter we present a detailed and thorough investigation of high-voltage I-V curves on Au and Pt ASCs formed under ultraclean conditions at low temperatures (4.2 K) using the MCBJ [see the inset of Fig. 1(b) and [13] for further experimental details]. We find that I-V curves on ASCs of Au are highly linear on a 100 mV scale, whereas for Pt distinct nonlinear effects exist as the conductance decreases with increasing voltage. First principles density functional theory (DFT) calculations confirm the different I-V behavior for Au and Pt, and we conclude that the difference is associated with the valence electron structure of the ASCs: Au has a closed d shell ($5d^{10}6s^1$) and the transport is dominated by a single, broad resonance of s character, while for Pt ($5d^96s^1$) also the d electrons participate. The general implications for other metals will be discussed.

To measure I-V curves we use a setup described in detail elsewhere [18]. In brief, it consists of a function generator supplying bias voltage and voltage bursts to the contacts. A calibrated, dc-20 MHz bandwidth homebuilt I-V converter is used together with a 100 Msamples, 10 bit resolution digital storage oscilloscope to capture the current response of the ASCs. When an ASC with a predefined conductance is formed, the function generator applies a voltage burst to the contact and an I-V curve is acquired. The burst consists of a triangular waveform with a frequency between 100–1000 Hz and an amplitude between 0.4–2 V superimposed on an offset of 50–250 mV. An I-V curve, i.e., a full burst cycle, is typically measured during 1–10 ms. Following each acquisition of an I-V curve the electrodes are brought

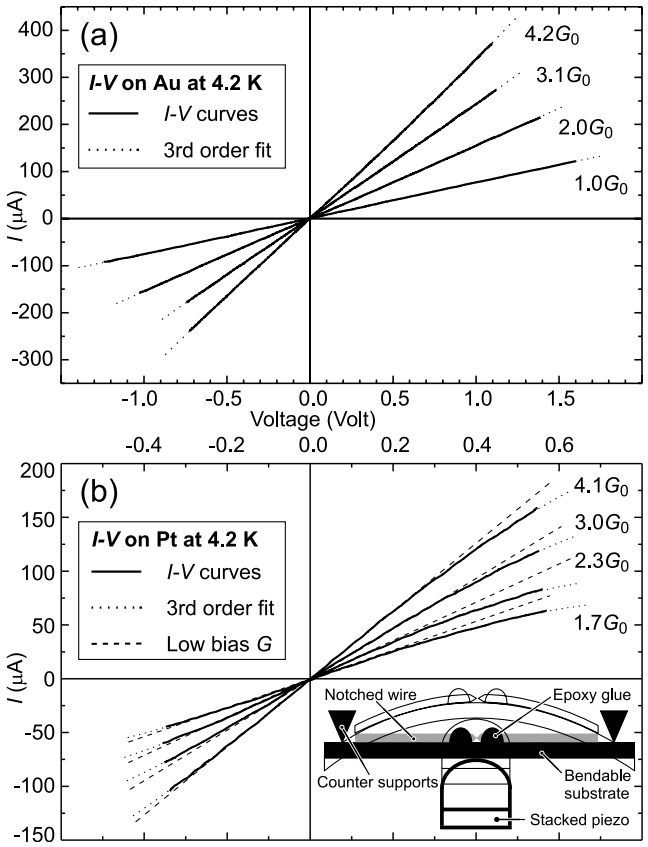

FIG. 1. Representative I-V curves on ASCs of (a) Au and (b) Pt. The I-V curves are fitted to the third-order polynomial from Eq. (1), and fits are plotted as dotted lines. Curves have been labeled by the low bias conductance G obtained from the fit. For Pt, the low bias conductance G for the curves is represented by the straight, dashed lines. Note that the voltage scale for Pt is a factor of 2.5 smaller than for Au. The inset in (b) shows a sketch of the MCBJ. The sample is made from a notched wire of Au or Pt with a purity of 99.999% and a diameter of 0.1 mm which is glued to a bendable substrate. The sample is mounted in a three-point bending device and placed in a vacuum pot which is lowered into liquid helium obtaining cryogenic vacuum. Then the wire is broken at the notch by bending the substrate with the center rod as indicated in the sketch. The break exposes clean fracture surfaces of bulk material from which ASCs can be formed and controlled using the stacked piezoelement.

back together until G rises above $50G_0$, then a new ASC is formed, ensuring that no two I-V curves are measured on contacts with the exact same atomic configuration. To include the most stable few-atom configurations in the experimental data set, we accept conductance values ranging from $0.9G_0$ to $5.0G_0$ for Au and from $1.5G_0$ to $5.0G_0$ for Pt, respectively. We avoid the exotic monatomic chain configurations known to exist for Au [12,13] and Pt [13] by stopping the elongation promptly if the conductance reaches a value associated with that of the monatomic contacts [$(0.9–1.1)G_0$ for Au, $(1.5–2.3)G_0$ for Pt].

In Fig. 1 typical I-V curves on ASCs for Au (a) and Pt (b) are shown. The I-V curves for Au are linear, i.e., Ohmic, whereas the I-V curves for Pt are clearly nonlinear. Monatomic Au contacts are very stable towards high voltages and often withstand burst amplitudes of 2 V and currents of more than 150 μA without breaking. Monatomic Pt contacts in general cannot withstand such high voltages; they typically break when the voltage exceeds 0.6 V. Because of the higher conductance, however, the current still reaches above 50 μA. Since this current is transmitted through one single atom, it results in an amazingly high current density of the order GA/mm^2.

To quantify the deviations from linearity we have fitted the I-V curves with the third-order polynomial

$$I(V) = GV + G'V^2 + G''V^3, \tag{1}$$

where the term G'' is used as an indicator of nonlinearity [8,9]. G represents the low bias conductance and G' describes the polarity dependence of the current due to asymmetries in the contact region. In Fig. 1 is shown the polynomial fit to the experimentally recorded I-V curves. For Pt we have furthermore added straight, dashed lines representing the low bias conductance G as guides to the eye [Fig. 1(b)]. Since the theoretical calculations are for a symmetric contact configuration with $G' \equiv 0$, we have for simplicity excluded clearly asymmetric I-V curves from the data analysis [19].

I-V curves from more than 2000 Au and Pt ASCs have been acquired and a (G, G'') scatter plot for fits to Eq. (1) is shown in Fig. 2. Several interesting differences between the Au and Pt results are observed. For monatomic Au contacts, G is clearly quantized consistent with reported conductance histograms [3,5,6,17]. Only 5% of the points with $G < 1.5G_0$ lie outside the conductance window from $0.9G_0$ to $1.1G_0$. The average for all points in this range

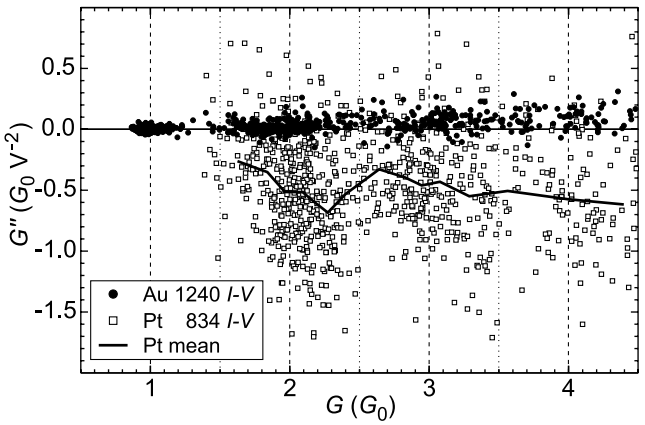

FIG. 2. Nonlinear term G'' vs low bias conductance G for Au and Pt ASCs. Each point represents a fit to Eq. (1) of one I-V curve on one ASC. There are points from 1240 Au and 834 Pt I-V curves. The solid curve represents the mean value of G'' for Pt. It is drawn through points found by averaging over 50 successive Pt points.

gives $G = 0.990(1)G_0$ and nearly zero nonlinear term $G'' = -0.0051(5)G_0\ \mathrm{V}^{-2}$. These results are in accordance with similar experiments at room temperature [9]. The density of points around $2G_0$ and $3G_0$ is also higher than average, but, as expected, the quantization in G gradually disappears with increasing conductance. In contrast, G for the monatomic Pt contact is never close to $1G_0$ and there is no sign of QC at $2G_0$. Although half of the points are situated between $1.5G_0$ and $2.5G_0$, only 30% of these lie in the interval from $1.9G_0$ to $2.1G_0$. The points spread over a large region both in G and G'', indicating a strong coupling of the conductance and the I-V behavior with the atomic configuration. The average value of G'' for Pt is represented by the solid curve drawn through the data in Fig. 2. The average is always negative, and the magnitude is at least 5 times larger than the similar average for Au [20]. The average decreases to a minimum of $-0.68G_0\ \mathrm{V}^{-2}$ around $G = 2.3G_0$ followed by a local maximum at $2.6G_0$ after which it decreases again with increasing G. This will be discussed in further detail below.

To obtain further insight into these experimental findings, we have calculated I-V curves using the TRANSIESTA program [21]. The method is based on DFT and takes the voltage bias and current explicitly into account in the self-consistent calculation of electronic density and potential. We have considered the symmetric atomic configuration depicted in Fig. 3(a) and varied the electrode-electrode distance. Our calculations show that the conductance (at zero voltage) of Au is quite constant with the variation in atom-electrode distance. G changes only from $1.1G_0$ to $1.0G_0$ as the distance increases from 2.65 to 3.5 Å. In contrast, Pt displays a strong variation in the conductance with a decrease from $2.1G_0$ to $1.1G_0$ over the same distance interval. This variation is in accordance with the often reported narrow histogram peak at $1G_0$ for Au [3,5,6,17] and the broad peak centered around $(1.5–2.0)G_0$ observed for Pt [6,13,15].

In Fig. 3(a) we show the calculated I-V corresponding to the atomic structure shown to the left with an atom-electrode distance of 2.9 Å. By fitting the calculated points to Eq. (1) we find that the Au I-V curve is indeed almost linear [22] with $(G, G'') = (1.05G_0, -0.03G_0\ \mathrm{V}^{-2})$, whereas the Pt I-V curve is nonlinear with $(G, G'') = (1.73G_0, -0.82G_0\ \mathrm{V}^{-2})$ in good agreement with the experimental findings.

According to the Landauer-Büttiker formalism [23] the conductance can be calculated from the total transmission as $G = G_0 T_{\mathrm{Tot}}$. The total transmission can be decomposed into nonmixing eigenchannels (T_n) as [24]

$$T_{\mathrm{Tot}}(E) = \sum_n T_n(E)\,. \qquad (2)$$

In Fig. 3(b) the calculated eigenchannel decomposition for Au and Pt is shown at both zero and finite bias. For finite bias the conductance (in units of G_0) is the average total transmission over the "voltage window" [dashed lines in Fig. 3(b)]. For zero voltage this amounts to the transmission at the Fermi energy (E_F). In the case of Au the transmission at 0 V is dominated by a single, broad channel of mainly s character resulting from a strong coupling between contact and electrode s orbitals. The slow variation of the channel transmissions with energy both at zero and finite bias results in a very linear I-V curve for Au [see left panel of Fig. 3(b)]. For Pt the situation is, however, quite different since we find four channels with significant contributions and a much stronger variation with energy for zero voltage [see right panel of Fig. 3(b)]. Note that the d_{yz}, d_{zx} channels are degenerate while the d_{xy} and $d_{x^2-y^2}$ channels are split due to the symmetry of the (100) electrodes. Additionally, the s and d_{z^2} orbitals combine at certain energies into two contributing channels. At finite bias a significant change in the channel structure is furthermore

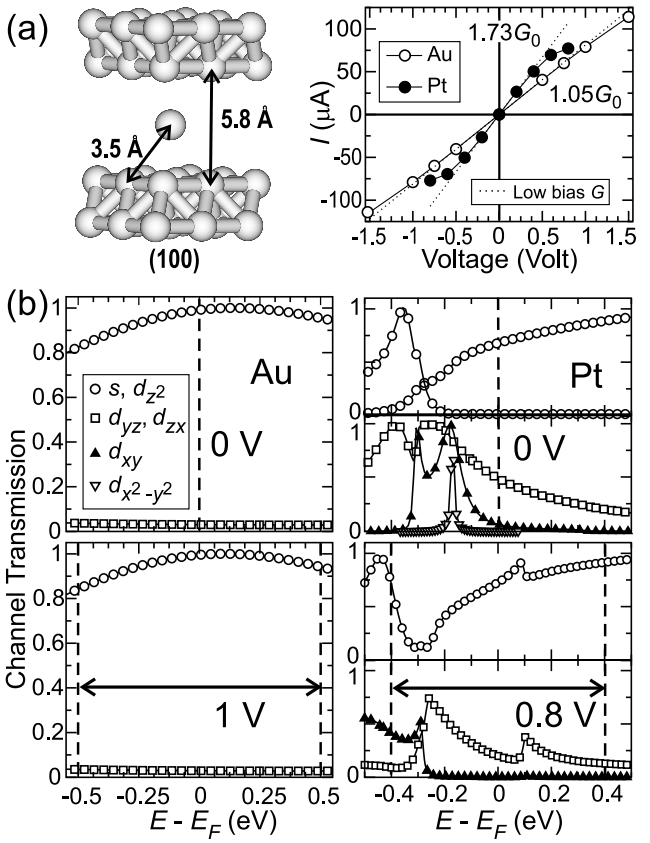

FIG. 3. (a) The atomic structure of a symmetric monatomic contact of Au and Pt between (100) electrodes and corresponding calculated I-V curves. (b) Eigenchannel decomposition of the total transmission through the atoms for Au for 0 and 1 V (left panels) and Pt for 0 and 0.8 V (right panels). Because of the complicated structure for Pt the graphs are split with the s, d_{z^2} channels in the upper window and the remaining channels in the lower window. The channels are labeled by their main orbital components (z is the direction perpendicular to the electrode surfaces). E_F is the Fermi energy at equilibrium. Dashed lines indicate the "voltage window" spanning $\pm\mathrm{eV}/2$ on each side of E_F.

found as the $\{d_{yz}, d_{zx}, d_{xy}\}$ derived channels become less transmitting and downshifted in energy and as the $d_{x^2-y^2}$ channel completely disappears. In contrast, the broader s-derived channel is not prone to the shift in potential, although it no longer splits into two channels. The result is a clearly nonlinear I-V curve.

The reason for the decrease in conductance with bias is the significant participation of the d electrons in the transport: The d electrons are more easily scattered by the voltage-induced potential, which in this case is of the same order of magnitude as the strength of the coupling to the electrodes. The same argument goes for the variation with atom-electrode distance. Here essentially the d contributions decrease as the distance increases.

These observations offer a possible explanation for the behavior of the Pt data in Fig. 2. The average of G'', represented by the solid curve, becomes more negative (increasing the nonlinearity) as G increases. In the regime from $(2.3-2.6)G_0$, however, a rapid rise in the average of G'' occurs—this is the conductance region in which monatomic contacts are replaced by two-atom contacts, explaining the lack of data. Below $2.3G_0$ the conductance decreases as the contact is stretched. As this happens the d electrons contribute less to the conductance, which explains why the nonlinearity is less pronounced at lower conductances. The pattern is repeated, although less clearly when G increases above $2.6G_0$. This corresponds to compressing a two-atom contact, increasing the contribution from the d electrons.

In conclusion, we have shown that the I-V behavior of atomic-size contacts is highly dependent on the valence electron structure of the appropriate electronic materials. Linear I-V curves can be expected only when exclusively s, p_z, and d_{z^2} electrons are involved in the transmission of the current, which is the case for noble and alkali metals. For most metals, however, open p or d shells will contribute to a complex electron structure which consequently leads to an equally complex eigenchannel decomposition. This will in general lead to nonlinear I-V curves as observed for Pt. The variety and richness in behavior observed here for the simplest atomic-scale conductors make it clear that the electronic structure of the electrode material itself will play a role in the design of nanoscale devices in the future.

We gratefully acknowledge financial support from The Center for Atomic-scale Materials Physics (CAMP) sponsored by the Danish National Research Foundation and from the EU network "Bottom up Nanomachines." M. B. acknowledges support from the Danish Natural Science Research Council. We thank Yves Noat for fruitful discussions.

*Corresponding author.
Email address: fbe@phys.au.dk

[1] For a review, see J. M. van Ruitenbeek, in *Metal Clusters on Surfaces: Structure, Quantum Properties, Physical Chemistry, Cluster Physics*, edited by K.-H. Meiwes-Broer (Springer-Verlag, Heidelberg, 2000), Chap. 6, pp. 175–210.
[2] L. Olesen *et al.*, Phys. Rev. Lett. **72**, 2251 (1994); L. Olesen *et al.*, *ibid.* **74**, 2147 (1995).
[3] B. Ludoph and J. M. van Ruitenbeek, Phys. Rev. B **61**, 2273 (2000).
[4] J. M. Krans *et al.*, Nature (London) **375**, 767 (1995).
[5] M. Brandbyge *et al.*, Phys. Rev. B **52**, 8499 (1995).
[6] C. Sirvent *et al.*, Phys. Rev. B **53**, 16 086 (1996).
[7] J. I. Pascual *et al.*, Science **267**, 1793 (1995).
[8] J. L. Costa-Krämer *et al.*, Phys. Rev. B **55**, 5416 (1997).
[9] K. Hansen *et al.*, Appl. Phys. Lett. **77**, 708 (2000).
[10] H. Mehrez *et al.*, Phys. Rev. B **65**, 195419 (2002).
[11] E. Scheer *et al.*, Nature (London) **394**, 154 (1998); B. Ludoph *et al.*, Phys. Rev. Lett. **82**, 1530 (1999).
[12] A. I. Yanson *et al.*, Nature (London) **395**, 783 (1998).
[13] R. H. M. Smit *et al.*, Phys. Rev. Lett. **87**, 266102 (2001).
[14] J. M. Krans *et al.*, Phys. Rev. B **48**, 14 721 (1993).
[15] Y. Noat *et al.* (to be published).
[16] K. Yuki, S. Kurokawa, and A. Sakai, Jpn. J. Appl. Phys. **39**, 4593 (2000).
[17] H. Yasuda and A. Sakai, Phys. Rev. B **56**, 1069 (1997).
[18] K. Hansen *et al.*, Rev. Sci. Instrum. **71**, 1793 (2000).
[19] In order to remove the asymmetric I-V curves, we use $|G'/G|$ as a selection criterion. In this way we set an upper limit for the percentage of asymmetry. Curves with $|G'/G| > 0.025\ \mathrm{V}^{-1}$ for Au and $|G'/G| > 0.05\ \mathrm{V}^{-1}$ for Pt are excluded. The lower value for Au is due to the higher stability of ACSs for Au compared to Pt. For both metals about 40% of the acquired curves fulfill the criterion. Although only asymmetric contacts can have large values of G', the opposite cannot be stated since an asymmetric contact might have G' close to zero.
[20] Although the mean value for Au is close to zero, we note that at higher G the Au data have a clear bias towards positive G''. Although not fully understood, it is most likely an effect of increasing electron tunneling as the contact size increases; see A. García-Martín *et al.*, Ultramicroscopy **73**, 199 (1998). We have not included the direct tunneling between the electrodes in our DFT calculations.
[21] M. Brandbyge *et al.*, Phys. Rev. B **65**, 165401 (2002). Here we use the same parameters except the orientation of the electrodes is (100) instead of (111). J. M. Soler *et al.*, J. Phys. Condens. Matter **14**, 2745 (2002).
[22] The electronic structure (projected band gap) of the (111) electrode itself yields a nonlinear I-V curve also for Au; see M. Brandbyge, N. Kobayashi, and M. Tsukada, Phys. Rev. B **60**, 17 064 (1999). The (100) and (110) electrodes yield linear I-V curves for Au [9], and more realistic, somewhat disordered electrodes—as in the experiment—will most likely also belong to this same category.
[23] D. S. Fisher and P. A. Lee, Phys. Rev. B **23**, 6851 (1981); M. Büttiker *et al.*, *ibid.* **31**, 6207 (1985); M. Büttiker, IBM J. Res. Dev. **32**, 63 (1988).
[24] M. Brandbyge, M. R. Sørensen, and K. W. Jacobsen, Phys. Rev. B **56**, 14 956 (1997).